

# Chirped Brillouin dynamic gratings for storing and compressing light

Herbert G. Winful<sup>1,2,\*</sup>

<sup>1</sup>Centre for Ultrahigh bandwidth Devices for Optical Systems (CUDOS), School of Physics, University of Sydney, Sydney, NSW 2007, Australia

<sup>2</sup>Department of Electrical Engineering and Computer Science, University of Michigan, Ann Arbor, MI 48109, USA  
[arrays@umich.edu](mailto:arrays@umich.edu)

**Abstract:** We demonstrate theoretically that chirped dynamic gratings can be created in optical fibers through stimulated Brillouin scattering with frequency-chirped “signal” and “write” pulses. When the grating is interrogated with a third pulse of the opposite chirp, a compressed signal pulse is retrieved. This provides a method to regenerate stored pulses and enhance signal levels for communications applications.

©2013 Optical Society of America

**OCIS codes:** (190.2055) Dynamic gratings; (290.5900) Scattering, stimulated Brillouin; (320.5520) Pulse compression; (060.4370) Nonlinear optics, fibers; (050.1590) Chirping.

---

## References and links

1. K. Y. Song, W. Zou, Z. He, and K. Hotate, “All-optical dynamic grating generation based on Brillouin scattering in polarization-maintaining fiber,” *Opt. Lett.* **33**(9), 926–928 (2008).
2. Z. Zhu, D. J. Gauthier, and R. W. Boyd, “Stored light in an optical fiber via stimulated Brillouin scattering,” *Science* **318**(5857), 1748–1750 (2007).
3. S. Chin and L. Thévenaz, “Tunable photonic delay lines in optical fibers,” *Laser Photon. Rev.* **6**(6), 724–738 (2012).
4. Y. Dong, X. Bao, and L. Chen, “Distributed temperature sensing based on birefringence effect on transient Brillouin grating in a polarization-maintaining photonic crystal fiber,” *Opt. Lett.* **34**(17), 2590–2592 (2009).
5. J. Sancho, N. Primerov, S. Chin, Y. Antman, A. Zadok, S. Sales, and L. Thévenaz, “Tunable and reconfigurable multi-tap microwave photonic filter based on dynamic Brillouin gratings in fibers,” *Opt. Express* **20**(6), 6157–6162 (2012).
6. F. Ouellette, “Dispersion cancellation using linearly chirped Bragg grating filters in optical waveguides,” *Opt. Lett.* **12**(10), 847–849 (1987).
7. G. P. Agrawal, *Nonlinear Optics*, 5th Ed. (Academic Press, San Diego, 2013), Ch. 9.
8. Z. Zhang, X. Zhou, L. Lan, and Y. Liu, “Performance analysis of optical buffering based on stimulated-Brillouin-scattering-induced acoustic excitation in an optical fiber,” *Opt. Commun.* **285**(24), 5378–5383 (2012).
9. Y. Ding, L. Bao, and J. Li, “Pulse compression effect based on stimulated Brillouin scattering light storage in optical fiber,” *Optik (Stuttg.)* **122**(24), 2172–2175 (2011).
10. J. R. Klauder, A. C. Price, S. Darlington, and W. J. Albersheim, “The theory and design of chirp radars,” *Bell Syst. Tech. J.* **39**, 745–808 (1960).
11. E. J. R. Kelleher, J. C. Travers, E. P. Ippen, Z. Sun, A. C. Ferrari, S. V. Popov, and J. R. Taylor, “Generation and direct measurement of giant chirp in a passively mode-locked laser,” *Opt. Lett.* **34**(22), 3526–3528 (2009).
12. M. Baldo, G. E. Town, and M. Romagnoli, “Generation of highly chirped pulses in a diode-pumped optical fiber laser,” *Opt. Commun.* **140**(1-3), 19–22 (1997).
13. Y. Cao, P. Lu, Z. Yang, and W. Chen, “An efficient method of all-optical buffering with ultra-small core photonic crystal fibers,” *Opt. Express* **16**(18), 14142–14150 (2008).
14. R. Pant, C. G. Poulton, D. Y. Choi, H. Mcfarlane, S. Hile, E. B. Li, L. Thévenaz, B. Luther-Davies, S. J. Madden, and B. J. Eggleton, “On-chip stimulated Brillouin scattering,” *Opt. Express* **19**(9), 8285–8290 (2011).
15. R. Pant, E. B. Li, C. G. Poulton, D. Y. Choi, S. Madden, B. Luther-Davies, and B. J. Eggleton, “Observation of Brillouin dynamic grating in a photonic chip,” *Opt. Lett.* **38**(3), 305–307 (2013).

---

## 1. Introduction

In stimulated Brillouin scattering, a light wave at angular frequency  $\omega_1$  can mix with a counter-propagating wave at a lower frequency  $\omega_2$  to drive a sound wave through the process of electrostriction if the two frequencies differ by the Brillouin shift  $\Omega_B$ . Through the photoelastic effect this sound wave creates a spatial modulation of the refractive index - a dynamic grating [1] that can reflect coherently another light wave at the appropriate

frequency. In the reflection process, part of the original light energy used to create the grating is transferred to the reflected wave. In 2007, Zhu, et al [2] showed that if the higher-frequency pump is considered a “data” pulse and the counter-propagating lower-frequency pulse a “write” pulse, the information carried by the “data” pulse is stored in the acoustic wave during the grating writing process. When this grating is interrogated by a delayed version of the “write” pulse, the information stored in the acoustic wave can be retrieved in the form of a fourth pulse at the original frequency of the “data” pulse. Clearly this process could form the basis for an optical buffer in fiber-optic communications systems. Other applications of the dynamic grating induced by SBS include controllable delay lines [3], distributed sensing [4], and microwave photonic filtering [5]. While the applications of dynamic gratings have been well explored, the possibility of creating chirped dynamic gratings, i.e. dynamic gratings whose period varies in a prescribed manner with distance, has not yet been discussed. In the field of fiber-optic communications, chirped fiber Bragg gratings play an important role as dispersion compensators and pulse shapers, and have made it possible to extend the reach of communications systems [6]. The introduction of chirp into the field of dynamic gratings should likewise open up many new applications.

Here we show that chirped Brillouin dynamic gratings (CBDG’s) can be written by chirped counter-propagating “data” and “write” pulses in an optical fiber. When interrogated by a delayed “read” pulse of the opposite chirp, a compressed “data” pulse is retrieved. The scheme provides a simple means of restoring signal levels that may have been degraded upon storage. The frequency chirps of the “data”, “write”, and “read” pulses can be regarded as a “chirp code” that provides an additional degree of freedom for signal processing and information storage and for the coherent control of stimulated Brillouin scattering.

## 2. Operating principle

The geometry of the interaction is shown in Fig. 1. A “signal” pulse at carrier frequency  $\omega_0$  interacts with a counter-propagating “write” pulse at carrier frequency  $\omega_0 - \Omega_B$ , where  $\Omega_B$  is the Brillouin angular frequency shift. Both pulses have the same linear frequency sweep, so that their complex amplitudes at the input ends can be written

$$A_1(z = 0, t) = A_{10} \exp\left[-\frac{1 + iC_1 t^2}{2 \tau_1^2}\right], \quad (1a)$$

$$A_2(z = L, t) = A_{20} \exp\left[-\frac{1 + iC_2 t^2}{2 \tau_2^2}\right], \quad (1b)$$

where, for simplicity, we have taken Gaussians with a  $1/e$  intensity half-width  $\tau_j$  and a chirp parameter  $C_j$ . The instantaneous frequencies of the pulses are then given by

$$\omega_1 = \omega_0 + (C_1 / \tau_1^2)t,$$

$$\omega_2 = \omega_0 - \Omega_B + (C_2 / \tau_2^2)t.$$

Where the pulses overlap in the fiber an acoustic grating will be formed if the difference in instantaneous frequency equals the Brillouin shift  $\Omega_B$  and their phases are correlated. Since the instantaneous frequency of the pulses is being chirped in time, the spatial period of the acoustic grating, which depends on the pulse frequency, will be similarly chirped in space. In creating the grating, energy from the signal (high frequency) pulse is transferred to the “write” (low frequency) pulse and to the acoustic grating. This chirped dynamic grating contains information from the signal pulse. The strength of the grating will decay exponentially in time with a  $1/e$  lifetime given by the acoustic phonon lifetime  $\tau_b$ . After a

controllable delay time  $T_s$ , a chirped “read” pulse with the same propagation direction and nominal carrier frequency  $\omega_0 - \Omega_B$  as the “write” pulse is launched into the fiber with its complex amplitude

$$A_3(z = L, t) = A_{30} \exp \left[ -\frac{1 + iC_3}{2} \frac{t^2}{\tau_3^2} \right]. \quad (1c)$$

The interaction of the “read” pulse with the acoustic grating results in the retrieval of the original signal pulse, an anti-Stokes process that can be seen as a reflection by the dynamic grating. If the chirp of the “read” pulse is the inverse of the chirps of the signal and “write” pulses, the result will be a highly compressed retrieved pulse owing to the delay equalization provided by the chirped grating.

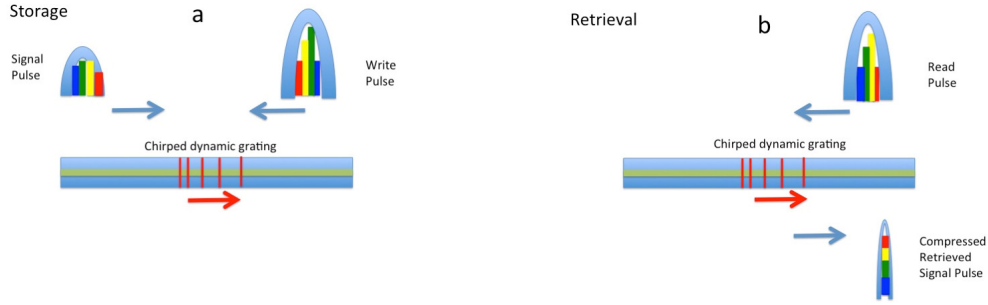


Fig. 1. (a) Storage of a chirped signal pulse through the formation of a chirped acoustic grating with a similarly chirped “write” pulse. (b) Retrieval of compressed signal by interrogating grating with oppositely chirped “read” pulse.

### 3. Formation of chirped Brillouin dynamic gratings

The interaction between light and sound in stimulated Brillouin scattering is described by the following coupled equations [2,7,8]:

$$\frac{\partial A_1}{\partial z} + \frac{n}{c} \frac{\partial A_1}{\partial t} = -\frac{g_B}{2A_{eff}} \tilde{Q} A_2, \quad (2a)$$

$$-\frac{\partial A_2}{\partial z} + \frac{n}{c} \frac{\partial A_2}{\partial t} = \frac{g_B}{2A_{eff}} \tilde{Q}^* A_1, \quad (2b)$$

$$2\tau_B \frac{\partial \tilde{Q}}{\partial t} + \tilde{Q} = A_1 A_2^*. \quad (2c)$$

Here  $A_1$  and  $A_2$  are the slowly-varying envelopes of the signal and “write” pulses, normalized so that  $|A_i|^2$  is power in watts; the variable  $\tilde{Q}$  is the amplitude of the acoustic density wave also normalized so that it has a value of watts;  $g_B$  is the Brillouin intensity gain coefficient (m/W),  $\tau_B$  is the acoustic lifetime,  $A_{eff}$  is the fiber effective area, and  $n$  is the fiber modal refractive index. In writing down these equations (see Appendix) we have dropped terms that describe linear loss and the nonlinear effects of self- and cross-phase modulation. For the short fibers considered here, loss is unimportant and the nonlinear index contribution is insignificant at the power levels of interest. We have checked that inclusion of the nonlinear index has no effect on the results presented here.

We first consider the formation of a uniform dynamic grating and compare its properties with that of a chirped grating. For a uniform grating we take the frequency chirp parameters in the signal and “write” pulses as  $C_1=C_2=0$ , while for a chirped grating we set  $C_1=C_2=-3$ . The strength of the grating is given by the magnitude of the acoustic vibration  $\tilde{Q}$ . The grating spatial distribution is essentially the convolution of the two pulses as they sweep through each other. The derivative of the phase of  $\tilde{Q}$  yields the local spatial frequency shift. For these simulations we use parameters from Zhu, et al [2] for their high-nonlinearity fiber:  $L = 5$  m,  $\tau_B = 3.4$  ns,  $g_B = 1.78 \times 10^{-11}$  m/W,  $\lambda = 1.55$   $\mu\text{m}$ ,  $n = 1.5$ , and fiber effective area  $A_{eff} = 11$   $\mu\text{m}^2$ . The signal and “write” pulses have FWHM’s of 2 ns and 1.5 ns respectively and peak powers of 10 mW and 100 W. Equations (2) were integrated numerically subject to the boundary conditions defined in Eqs. (1). Figure 2 shows a snapshot of  $|\tilde{Q}|$  taken at the instant when the two pulses exit the fiber. Clearly the dynamic grating is naturally tapered with a Gaussian-like profile. This is similar to the apodization of fiber Bragg gratings, a process that reduces or eliminates side lobes in the reflection spectrum. It is seen that the grating formed with chirped pulses is much narrower than the one formed with unchirped pulses. This is because the frequency sweeps ensure that the pulses are correlated over a much smaller region. The amplitude is also higher because there is a more efficient

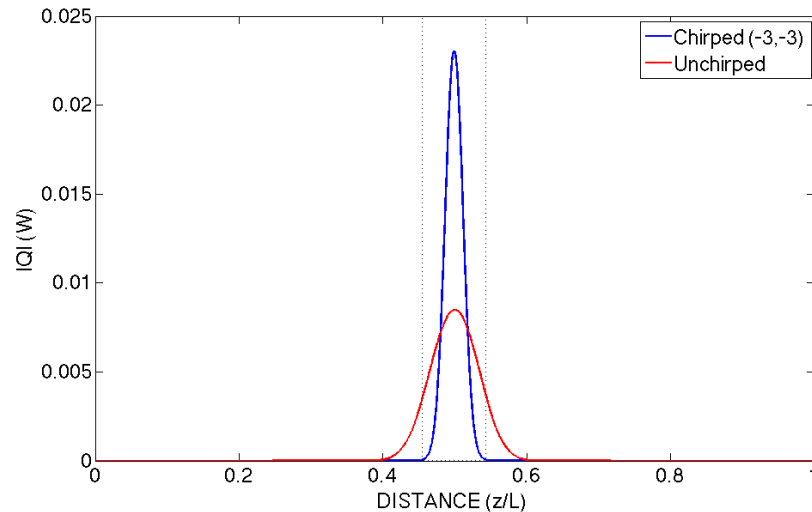


Fig. 2. Grating strength versus distance for gratings formed by chirped (blue) and unchirped (red) pulses. Note the greater localization of the grating formed with chirped pulses. The dotted lines demarcate the region occupied by the grating.

transfer of energy from the chirped signal pulse to the grating and to the “write” pulse. With unchirped pulses the grating formed by the early part of the “write” pulse is depleted by the later part in an anti-Stokes process that returns energy from the “write” pulse and acoustic wave to the signal pulse. The greater localization of the dynamic grating that is achievable with chirped pulses should be an advantage in distributed sensing applications, making possible greater spatial resolution.

To see whether the grating is chirped we plot in Fig. 3 the phase of  $\tilde{Q}$  as a function of position along the fiber. For the grating written with unchirped pulses (red) the phase is constant across the length of the grating. In the grating written with chirped pulses (blue) we see a large region of beat oscillations where the phases of the two pulses are uncorrelated.

Because the grating amplitude is essentially zero in those regions, these oscillations have no effect on grating properties. In the region where the grating exists ( $0.46 < z/L < 0.54$ ), the phase reveals what appears to be a quadratic dependence on distance. We examine the grating phase more closely in Fig. 4, which zooms in on the portion occupied by the grating.

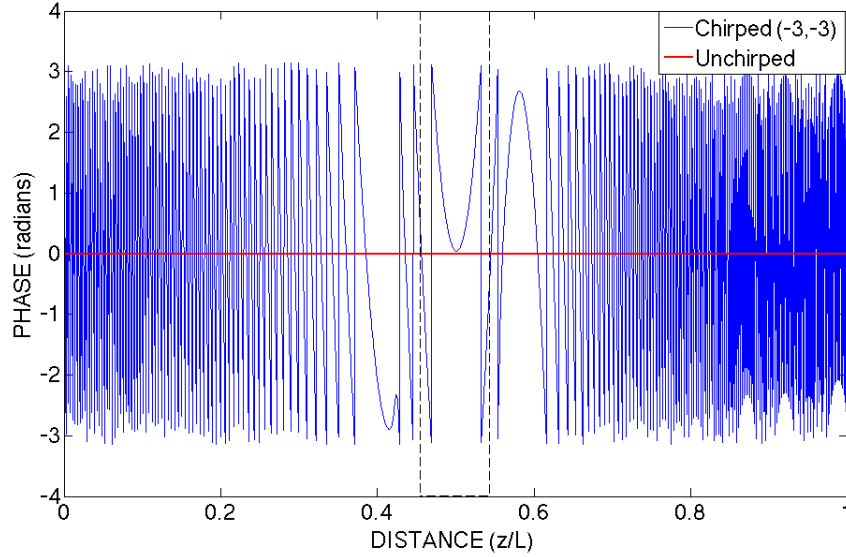


Fig. 3. Grating phase for chirped (blue) and unchirped (red) pulses. The phase of the unchirped grating is constant. The dotted lines demarcate the region where the grating has finite amplitude.

The expanded view and a fit to the calculated phase confirm that there is indeed a quadratic phase. The quadratic phase profile implies a linear chirp of the spatial frequency that can be expressed as

$$\Delta K(z) = d\phi/dz,$$

or, equivalently, as a change in the grating period

$$\frac{\Delta\Lambda(z)}{\Lambda} = -\frac{\Delta K(z)}{K},$$

where  $K = 2\pi/\Lambda$  and  $\Lambda = \lambda/2n$ . From the quadratic fit, we find that the fractional change of the grating period over its spatial extent is  $\Delta\Lambda/\Lambda \approx 2 \times 10^{-5}$ . While this may seem small, it is consistent with the fractional bandwidth of the chirped pulse, which is  $\Delta\nu/\nu \sim 10^{-5}$ . This demonstrates clearly that chirped dynamic gratings can be created through stimulated Brillouin scattering. These gratings are reconfigurable and the sign of the chirp can be easily changed by reversing the chirp on the signal and “write” pulses. This means that both positively and negatively chirped pulses can be compressed in the same fiber simply by flipping the signs of the “read” and “write” pulses.

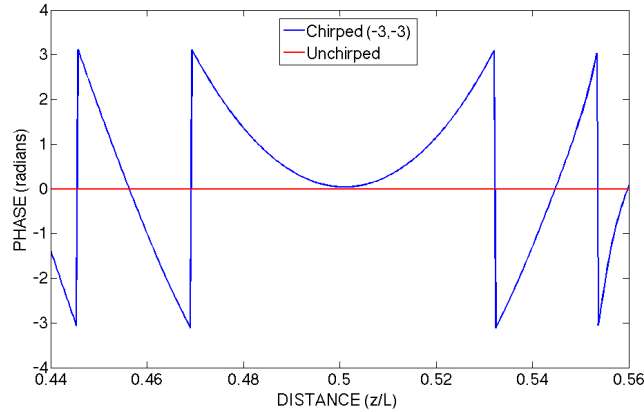


Fig. 4. Expanded view of the phase profile in the region where the grating has finite amplitude. A fit to the calculated profile confirms the creation of a quadratic phase.

#### 4. Simulation of pulse compression by chirped Brillouin gratings

The formation of the acoustic grating through stimulated Brillouin scattering is essentially the storage of light in the form of an acoustic excitation. In reality only a small fraction of the signal beam's energy is stored as sound while the greatest portion is transferred to the counter-propagating write pulse. The higher frequency signal acts as a pump for the Stokes-shifted "write" beam. Efficient light storage and grating formation requires that the signal be completely depleted. The signal can be retrieved if the dynamic grating is interrogated with a "read" pulse of the same frequency and direction of propagation as the "write" pulse. This interrogation should occur before the grating decays away. In the experiment of Zhu, et al, the retrieved pulse amplitudes were about an order of magnitude lower than that of the original signal and significant broadening was also observed. A scheme to restore the pulse height and width would be of interest.

Chirped fiber Bragg gratings are used to compensate for dispersion-induced pulse broadening in fiber-optic communications systems [6]. Here we show that chirped Brillouin dynamic gratings can also function as dispersion compensators and pulse compressors in optical storage applications. The approach is straightforward: simply interrogate the chirped grating formed in the writing phase with a "read" pulse whose chirp is opposite in sign to the chirp of the signal and "write" pulses. The chirped grating acts as a matched filter and delay-equalizer for the "read" pulse, leading to pulse compression. Figure 5 shows a simulation in which a "read" pulse is sent into the fiber 4 ns after the launching of the signal pulse. We compare the retrieved pulse for different values of the chirp parameter  $C$ . In the figure each pulse is labeled by the chirp code  $(C_{\text{signal}}, C_{\text{write}}, C_{\text{read}})$  that produced it. In the case of zero chirp, i.e.  $[C] = (0,0,0)$ , there is a large amount of undepleted signal energy that exits the fiber before the read pulse arrives. This is because the bandwidth of the "write" and "read" pulses is insufficient to fully capture the information stored in the data pulse. The amount of energy released by the "read" pulse after a delay of 4 ns is negligible. If a chirp of +3 is applied to only the control ("write" and "read") pulses, i.e.  $[C] = (0,3,3)$ , the increased bandwidth of the control pulses results in faithful storage and reproduction of the signal pulse, as can be seen in the green curve. There is no compression, however. With  $[C] = (3,3,-3)$ , i.e. when the "read" pulse chirp is the negative of the signal and "write" chirps, we see (blue curve) that the retrieved pulse is compressed by about a factor of 2 and its amplitude enhanced. To confirm the role of the sign of the chirp, Fig. 4 also includes a plot with the chirp code  $[C] = (3,3,3)$  which shows that there is no compression if the chirp of the "read" pulse has the same sign as that of the "write" and signal pulses. The chirp code has the property that  $[C]$  and  $-[C]$  result in the same compressed retrieved pulse. This is a result of time-reversal symmetry.

The amount of compression does increase with the strength of chirp. However, for large chirp magnitudes there is also an increase in the amount of undepleted (wasted) signal energy which means the pulse storage efficiency begins to drop. This is because the chirp across the pulse is so strong that the region over which the pulses are correlated is very small. These simulations confirm that chirped dynamic Brillouin gratings can be used to store light pulses and release them as highly compressed replicas if the “read” pulse has an opposite chirp to that of the “write” pulses.

The use of chirped pulses in pulse storage has been previously considered [8,9]. However, in those papers the chirp was applied only to the control pulse for the purpose of increasing its bandwidth while “data” pulse was left unchirped. Only positive chirps were considered and no pulse compression was seen in [8] and insignificant narrowing (from 2 ns down to 1.73 ns) was reported in [9]. No mechanism was advanced for this narrowing. Our approach here is based on the matched-filter concepts developed for chirp radar in the 1950’s [10]. While we have focused on linear chirps in this paper, it is clear that more complicated chirps such as quadratic and higher order chirps can also be implemented for particular applications.

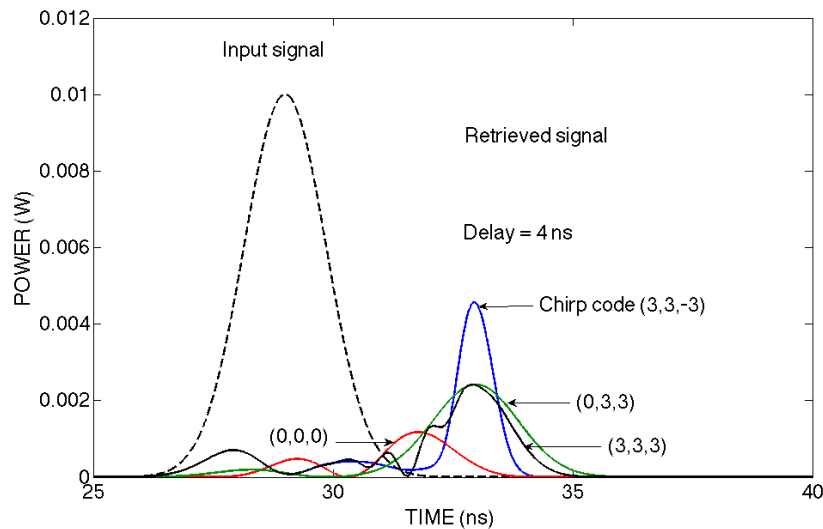


Fig. 5. Retrieved pulses after a 4 ns delay showing the significant compression achievable with a chirped Brillouin dynamic grating and “read” pulses of opposite chirp (blue curve). The output labeled (0,0,0) is simply the unused portion of an unchirped signal pulse. The input signal (dashed curve) is translated to the output by the 25 ns transit time.

## 5. Experimental considerations

We now consider the possibility of experimental verification of the concepts proposed in this paper. Because the acoustic lifetime is a few nanoseconds, efficient creation of Brillouin dynamic gratings requires pulses that are longer than about a nanosecond. The pulse chirp parameter  $C$  is the most important quantity that controls the formation of chirped dynamic gratings. A value of  $C = 1$  for a nanosecond pulse corresponds to a 1-GHz frequency sweep in 1 nanosecond. This chirp of  $10^{18}$  Hz/s is three orders of magnitude higher than what is achievable through direct current modulation of a diode laser or through the use of an external electro-optic modulator. Fortunately it has been demonstrated that extremely large chirps are obtainable in nanosecond mode locked lasers that operate in the positive dispersion regime. Indeed, chirps as large as 0.14 nm/ns (equivalent to 42 GHz/ns) have been measured at 1.059  $\mu\text{m}$  in ytterbium fiber lasers mode locked with single-walled carbon nanotubes as saturable absorbers [11]. A diode-pumped mode locked fiber laser yielded a chirp of order 1 THz/ns [12]. The use of grating stretchers can also provide large amounts of both positive and

negative chirp, while dispersive nonlinear propagation offers a means of stretching picosecond pulses into strongly chirped nanosecond pulses.

The power requirements are not excessive. In the simulations presented here we have used a control power of 100 W as done in the experiment of Zhu, et al. By careful design, it has been shown in simulations that the power can be reduced to the range of 2 W in small-core photonic crystal fibers [13]. Ultimately, the use of materials such as chalcogenide glasses with high Brillouin gains should make it possible to observe these phenomena with low power lasers on centimeter-scale photonic chips [14,15].

## 6. Conclusion

In this paper we have shown that chirped Brillouin dynamic gratings can be created by using chirped counter-propagating pump and Stokes pulses. Information transferred to the acoustic wave during the writing process can be recovered in the form of a compressed pulse by interrogating the grating with a pulse of the opposite chirp. The compression of the retrieved pulses enhances their amplitude and leads to improvements in signal-to-noise ratio. Our scheme makes it possible to create dynamically reconfigurable chirped gratings for dispersion compensation. It should also improve the spatial resolution of distributed sensors that rely on Brillouin dynamic gratings. The introduction of chirp as an extra degree of freedom should open up possibilities for chirp coding and for the coherent control of stimulated Brillouin scattering.

## Appendix

The general 3-wave equations for the interaction between pump ( $A_1$ ), Stokes ( $A_2$ ), and acoustic waves ( $Q$ ) are [7]

$$\frac{\partial A_1}{\partial z} + \frac{n}{c} \frac{\partial A_1}{\partial t} = i \kappa_1 Q A_2 - \frac{\alpha}{2} A_1 + i \gamma (|A_1|^2 + 2|A_2|^2) A_1, \quad (\text{A1})$$

$$-\frac{\partial A_2}{\partial z} + \frac{n}{c} \frac{\partial A_2}{\partial t} = i \kappa_1 Q^* A_1 - \frac{\alpha}{2} A_2 + i \gamma (|A_2|^2 + 2|A_1|^2) A_2, \quad (\text{A2})$$

$$\frac{\partial Q}{\partial t} + v_A \frac{\partial Q}{\partial z} = - \left[ \frac{1}{2} \Gamma_B + i (\Omega_B - \Omega) \right] + i \kappa_2 A_1 A_2^*, \quad (\text{A3})$$

with the coupling constants

$$\kappa_1 = \frac{\omega_0 \gamma_e \langle F_p^2 F_A \rangle}{2nc \rho_0 \langle F_p^2 \rangle} \text{ and } \kappa_2 = \frac{\omega_0 \gamma_e \langle F_p^2 F_A \rangle}{2c^2 v_A \langle F_A^2 \rangle A_{eff}}$$

Here  $v_A$  is the acoustic velocity,  $\alpha$  the intensity loss coefficient,  $\Omega = \omega_1 - \omega_2$ ,  $\Omega_B$  is the Brillouin shift,  $\Gamma_B = 1/\tau_B$ ,  $\rho_0$  the average material density,  $\gamma_e$  the electrostrictive constant,  $\gamma = n_2 \omega_1 / c$ ,  $n_2$  the nonlinear index coefficient,  $F_p$  and  $F_A$  the transverse profiles of the pump and acoustic modes, with the angular brackets indicating an integral over the fiber cross section.

To obtain Eqs. (2) in the text, we assume operation near the Brillouin gain peak  $\Omega = \Omega_B$ , that the acoustic phonons are heavily damped so that  $\partial Q / \partial z \rightarrow 0$  in (A3), that the optical intensity loss is negligible, and that the effects of the nonlinear index are insignificant. We further normalize the acoustic wave amplitude  $Q$  ( $kg/m^3$ ) so that the new variable  $\tilde{Q} = Q / 2i \kappa_2 \tau_B$  has dimensions of watts. The peak Brillouin gain is given by  $g_B = 4\kappa_1 \kappa_2 \tau_B$ .

### **Acknowledgment**

This work was done while HW was on sabbatical at the Center for Ultrahigh bandwidth Devices for Optical Systems, University of Sydney. He thanks Prof. Ben Eggleton for providing the stimulating environment that made this research possible.